HOKKAIDO UNIVERSITY

Title	Highly selective and efficient photocatalytic reduction of nitrate in water by a tandem reaction system consisting of Pt/TiO2 and SnPd/Al2O3: A comparative study of the tandem reaction system with a typical semiconductor photocatalyst, SnPd/TiO2
Author(s)	Hirayama, Jun; Kamiya, Yuichi
Citation	Journal of catalysis, 348, 306-313 https://doi.org/10.1016/j.jcat.2016.12.019
Issue Date	2017-04
Doc URL	https://hdl.handle.net/2115/73374
Rights	© 2017. This manuscript version is made available under the CC-BY-NC-ND 4.0 license http://creativecommons.org/licenses/by-nc-nd/4.0/
Rights(URL)	https://creativecommons.org/licenses/by-nc-nd/4.0/
Type	journal article
File Information	Revised manuscript (JCAT-16-1152).pdf

Hokkaido University Collection of Scholarly and Academic Papers : HUSCAP

Revised manuscript (JCAT-16-1152)

Highly selective and efficient photocatalytic reduction of nitrate in water by a tandem reaction system consisting of Pt/TiO_2 and $SnPd/Al_2O_3$: A comparative study of the tandem reaction system with a usual semiconductor photocatalyst $SnPd/TiO_2$

Jun Hirayama[a,b] and Yuichi Kamiya[a,*]

[a] Faculty of Environmental Earth Science, Hokkaido University, Nishi 5, Kita 10, Kita-ku, Sapporo, Hokkaido 060-0810, Japan

[b] Research Fellow of Japan Society for the Promotion of Science (JSPS), 5-3-1 Chiyoda-ku, Tokyo 102-0083, Japan

[*]Corresponding author

Yuichi Kamiya

E-mail: kamiya@ees.hokudai.ac.jp, Tel/Fax: +81-11-706-2217

Abstract

A tandem reaction system consisting of a photocatalyst (Pt/TiO_2) and a non-photocatalyst ($SnPd/Al_2O_3$) promoted the reduction of NO_3^- into gaseous products (mainly N_2) under light irradiation ($\lambda > 300$ nm) in the presence of glucose as a hole scavenger. Photocatalytic H_2 evolution ($2H^+ + 2e^- \rightarrow H_2$) proceeded over Pt/TiO_2, and conventional catalytic reduction of NO_3^- with H_2 ($NO_3^- + 5/2H_2 \rightarrow 1/2N_2 + 2H_2O + OH^-$) occurred over $SnPd/Al_2O_3$. We optimized the loading amount of Pt on TiO_2, the Sn/Pd ratio, the loading amount of SnPd on Al_2O_3, and the two catalyst dosages. The optimized tandem system gave a high reduction rate of NO_3^- and high selectivity for gas (94%) from the photocatalytic reduction of NO_3^- in water. On the other hand, a usual semiconductor photocatalyst $SnPd/TiO_2$ with an optimized Sn/Pd ratio and an optimized loading amount of SnPd bimetal on TiO_2 reduced NO_3^- at about two-thirds as fast as the tandem system and was less selective for gas (70%). The tandem system suppressed the wasted H_2 formation, resulting in high light use efficiency for the NO_3^- reduction (95%), which is defined as the ratio of electrons consumed for NO_3^- reduction to the total number of electrons consumed for both NO_3^- reduction and photocatalytic H_2 evolution, though the tandem and $SnPd/TiO_2$ systems consumed about the same total number of electrons. The tandem system has two advantages: (i) the Pt/TiO_2 and $SnPd/Al_2O_3$ subsystems can be separately designed to give highly efficient photocatalytic and catalytic reactions, respectively; and (ii) the reaction rates of photocatalytic and catalytic reactions can be easily controlled by changing the catalyst dosage in the reactor. Those advantages brought about a high reduction rate of NO_3^-, high selectivity for gas, and high light use efficiency for NO_3^- reduction in the photocatalytic reduction of NO_3^- in water.

Key words: Photocatalysis, Nitrate reduction, Pt/TiO_2, Tandem reaction system, Catalytic-function differentiation, Tin-palladium bimetal, Hydrogenation

1. Introduction

Photocatalytic reactions over semiconductor photocatalysts, such as TiO_2 and WO_3, proceed sequentially by the following steps: (i) adsorption of substrate onto the surface, (ii) photoabsorption forming photoexcited electrons (e^-) and holes (h^+) in the bulk, (iii) migration of e^- and h^+ to the surface, (iv) participation of e^- and h^+ in reduction and oxidation, respectively, with the substrates on the surface, and (v) recombination of unreacted e^- and h^+. For reactions in aqueous solution, water is included in the substrate in the steps of (i) and (iv). The observed rates of the chemical reactions, that is, the rates of reactant consumption and product formation, depend on the rates of these steps, unless radical chain reactions in solution or gas phase occur. The rates of steps (i), (ii), (iii), and (iv) positively influence the observed rate, whereas the rate of (v) negatively influences it, if those are involved in the rate determining step.

Generally, the photocatalytic activity of unmodified (bare) semiconductor photocatalysts is low, but the rate can be dramatically increased by modifying the semiconductor with a small amount of a metal [1–29], which is called a co-catalyst. One function of co-catalysts, such as Pt [1–5] and Pd [6–10], is to prolong the charge-separated state of photoexcited electrons and holes by the trapping of either electrons or holes on the co-catalyst [11]. In this way, the rate of (v) is decreased, although an excess of the co-catalyst increases the rate of recombination of e^- and h^+ [11]. Another function of co-catalysts is to activate substrate molecules via adsorption, which accelerates the rate of (iv): for example, NiO_x [12–16] and $Rh_{2-y}Cr_yO_3$ [17–19] for water splitting; Ag [20–22] for CO_2 reduction; and CuPd [23–26] for NO_3^- reduction. For the photocatalytic reduction of CO_2 or NO_3^- in water, the photocatalytic reduction of water (H^+) to form gaseous H_2 can occur in parallel with the target reaction over co-catalyst with low hydrogen overpotential like Pt and Pd [23, 27, 28]. Photocatalytic H_2 evolution lowers the photocatalytic performance for the target reaction as pointed out by Anderson [27, 28], because photoexcited electrons are wasted to form H_2, rather than reducing the substrates in water. Thus, H_2 production needs to be suppressed to enhance photocatalytic efficiency. Because both

reactions (H_2 evolution and the reduction of CO_2 or NO_3^-) proceed on the co-catalyst, the co-catalyst needs to have excellent adsorption of substrate molecules to preferentially promote the reduction of substrates rather than H_2 evolution. If the two functions of the co-catalyst, (prolonging the charge-separated state of photoexcited electrons and holes and activating substrate molecules) are maximized simultaneously by optimizing the design of the co-catalyst, including the choice of element, loading amount, crystalline structure, and particle size, then extremely high-performance semiconductor photocatalysts can be obtained. However, it is very difficult, in general, to achieve simultaneous maximization.

To overcome this difficulty, the use of a tandem reaction system has been proposed, in which the photocatalytic/catalytic functions are distributed to separate particles and those are reconstituted in the reaction mixture. Artificial Z-scheme photocatalytic water splitting [31–33], which affords H_2 and O_2, is a great example of function distribution over separate catalysts. In the Z-scheme photocatalytic system, O_2 and H_2 evolution sites are built on separate semiconductor photocatalysts (e.g., WO_3 for O_2 evolution and TaON for H_2 evolution), and the two catalysts are added to the reaction mixture with a redox shuttle between them.

We have previously reported a tandem reaction system consisting of a photocatalyst and non-photocatalyst (usual catalyst) for the photocatalytic reduction of NO_3^- in water (Figure 1(a)) [34–36]. In the tandem reaction system, H_2 is formed by a photocatalytic reaction over the photocatalyst (eq. 1), and this H_2 reduces NO_3^- in water over the non-photocatalyst (eq. 2):

$$2H^+ + 2e^- \rightarrow H_2 \quad (1)$$

$$NO_3^- + 5/2H_2 \rightarrow 1/2N_2 + 2H_2O + OH^- \quad (2)$$

In the tandem reaction system, the photocatalyst and non-photocatalyst can be developed independently to maximize their performance. In addition, the two reaction rates can be appropriately adjusted by changing the doses of the photocatalyst and non-photocatalyst in the

reaction mixture. Thus, the tandem reaction system has great potential to become a much better system for photocatalytic NO_3^- reduction in terms of both activity and selectivity than a conventional system of a semiconductor directly combined with a co-catalyst, which we call a single reaction system (Figure 1 (b)). Based on the concept described above, we have developed a tandem reaction system using a photocatalyst (Pt/TiO_2 [34, 35], $Pt/SrTiO_3$:Rh [36]) and a non-photocatalyst ($SnPd/Al_2O_3$) that shows high photocatalytic activity and excellent selectivity for gases, including N_2 and N_2O.

In the present study, we compared in detail the photocatalytic performance of a tandem reaction system consisting of a Pt/TiO_2 photocatalyst and a $SnPd/Al_2O_3$ non-photocatalyst with that of a single semiconductor photocatalyst, $SnPd/TiO_2$, to demonstrate superiority of the tandem reaction system. Before the comparison, the tandem and single reaction systems were comprehensively optimized. In particular, we focused on the reduction rate of NO_3^-, product selectivity, and light use efficiency for NO_3^- reduction. The photocatalytic reduction of NO_3^- in water is a promising method to purify groundwater polluted with NO_3^-, which is a serious global problem. In the purification of groundwater, the formation of ammonia and ammonium ions is undesirable due to their toxicity and so the reaction systems should have high selectivity for gaseous products, such as N_2 and N_2O, as well as high photocatalytic activity.

2 Experimental

2.1. Preparation of catalysts

AEROXIDE® TiO_2 P25 (Evonik) was used as a TiO_2 photocatalyst. Modification of TiO_2 with Pt was conducted by photodeposition. TiO_2 (2 g) was dispersed in distilled water (135 cm^3) and then CH_3OH (15 cm^3, Wako Pure Chemical Industries) and $H_2PtCl_6 \cdot 6H_2O$ (0.04 mol dm^{-3}, Wako Pure Chemical Industries) were added to the suspension. The suspension in a Pyrex glass cell was sparged with a stream of N_2 (15 cm^3 min^{-1}) for 30 min, and then irradiated using a 300 W Xe lamp (Optical Modulex, USHIO) for 3 h with stirring.

The suspension was centrifuged and the supernatant was replaced with distilled water (200 cm^3). The suspension was stirred for a few minutes and centrifuged again. This process was repeated three times. Finally, the catalyst powder was dried in air at 333 K overnight. The obtained catalyst is denoted Pt/TiO_2.

Supporting Sn and Pd on Al_2O_3 (AEROSIL®, Alu C) was conducted by incipient wetness impregnation. Al_2O_3 was heated in air at 523 K for 4 h before use. An aqueous solution of $PdCl_2$ (0.112 mol dm^{-3}, Wako Pure Chemical Industries) was dropped onto Al_2O_3 (2.0 g), and then the resulting wet solid was dried in air at 373 K overnight, followed by calcination in air at 523 K for 3 h. An aqueous solution of $SnCl_2 \cdot 2H_2O$ (0.172 mol dm^{-3}, Wako Pure Chemical Industries) was dropped onto the resulting solid, and then the wet solid was dried in air at 373 K overnight, followed by calcination in air at 523 K for 3 h. The obtained catalyst is denoted $SnPd/Al_2O_3$. When we pay attention to the molar ratio of Sn to Pd (Sn/Pd = *n*), the catalyst is written as Sn_nPd/Al_2O_3, in which *n* represents the Sn/Pd molar ratio. TiO_2 modified with Sn and Pd was prepared with a procedure similar to that for $SnPd/Al_2O_3$, and is denoted $SnPd/TiO_2$.

Just before the photocatalytic and non-photocatalytic reactions, $SnPd/Al_2O_3$ was reduced with $NaBH_4$ (Wako Pure Chemical Industries). To the aqueous suspension (30 cm^3) in which $SnPd/Al_2O_3$ was dispersed, $NaBH_4$ (molar ratio of $NaBH_4$/(Sn+Pd)=10) was added, and the suspension was stirred at room temperature for 30 min. The catalyst powder was filtered, washed with distilled water (ca. 200 cm^3), and then used in the reactions. The reduction of $SnPd/TiO_2$ was performed using a procedure similar to that for $SnPd/Al_2O_3$.

2.2. Photocatalytic reduction of NO_3^- in water

Photocatalytic reduction of NO_3^- in water was carried out in a Pyrex reaction vessel connected to a closed gas circulation system. The catalyst was suspended in an aqueous solution of KNO_3 (1.0 mmol dm^{-3}, 250 cm^3) containing glucose (100 mmol dm^{-3}, Wako Pure Chemical

Industries), and the suspension was stirred using a magnetic stirrer. The reaction mixture was thoroughly degassed with a vacuum pump and then placed under a He atmosphere (101.3 kPa). The light source was a 300 W Xe lamp covered with Pyrex glass (cut-off λ > 300 nm). The evolved gas was analyzed using on-line gas chromatography (He carrier gas, 3000 A Micro GC, Agilent Technologies) with columns of molecular sieves (for H_2, O_2, and N_2) and Porapak Q (for N_2O). The concentrations of NO_3^-, NO_2^-, and NH_4^+ in the reaction mixture were determined by using two ion chromatographs (IC2001, Tosoh).

2.3. Non-photocatalytic (catalytic) reduction of NO_3^- with H_2 in water

Non-photocatalytic, that is, conventional catalytic, reduction of NO_3^- with H_2 in water in the presence of $SnPd/Al_2O_3$ or $SnPd/TiO_2$ was carried out in a batch reactor at 298 K in the dark. The reaction mixture (250 cm^3, NO_3^- 1.0 mmol dm^{-3}) containing the catalyst was sparged with a stream of He (30 cm^3 min^{-1}) for 30 min. Then, gas was changed to a mixture of H_2 (0.5 atm) and CO_2 (0.5 atm) to start the reaction. A small portion of the reaction mixture was periodically withdrawn and was analyzed by ion-chromatography to determine the concentrations of NO_3^-, NO_2^-, and NH_4^+.

2.4. Photocatalytic H_2 evolution

Photocatalytic H_2 evolution from a reaction mixture with glucose was carried out using a procedure similar to that for the photocatalytic reduction of NO_3^- in water as described in Section 2.2, but there was no KNO_3 in the reaction mixture.

3. Results and discussion

3.1. Optimization of the tandem reaction system for photocatalytic reduction of NO_3^-

Figure 2 shows data of the photocatalytic reduction of NO_3^- in water under light irradiation for 4 h. Pt/TiO_2 alone without $Sn_{0.5}Pd/Al_2O_3$ showed negligible activity for the reduction of

NO_3^-, while H_2 gas was evolved (690 μmol) by a photocatalytic reaction ($2H^+ + 2e^- \rightarrow H_2$) consuming glucose as a hole scavenger. $Sn_{0.5}Pd/Al_2O_3$ alone in the absence of Pt/TiO_2 showed no activity for either NO_3^- reduction or H_2 evolution. In contrast, the tandem reaction system promptly reduced NO_3^- and 54% conversion was obtained at 4 h. The reaction with the tandem system did not form any harmful NO_2^- and the selectivity to NH_4^+ was less than 6%. A small amount of N_2O was formed at 4 h in the tandem reaction system. Because N_2O is a greenhouse gas, its formation should be prevented. In the tandem reaction system, N_2O was reduced into N_2 after additional reaction time (Figure S1) and thus its production does not matter much.

Even for the tandem reaction system, 20 μmol of H_2 gas (**A**) was formed at 4 h by the photocatalytic reaction. In addition, the estimated amount of H_2 required for NO_3^- reduction into each product was 365 μmol (**B**), which was calculated from the yields of N_2O, N_2, and NH_4^+ at 4 h based on eqs. 3-5.

$$NO_3^- + 5/2H_2 \rightarrow 1/2N_2 + 2H_2O + OH^- \quad (3)$$

$$NO_3^- + 2H_2 \rightarrow 1/2N_2O + 3/2H_2O + OH^- \quad (4)$$

$$NO_3^- + 4H_2 \rightarrow NH_4^+ + H_2O + 2OH^- \quad (5)$$

The sum of **A** and **B** was 385 μmol at 4 h for the tandem reaction system. In a separate experiment, we determined that the amount of H_2 gas evolved under conditions similar to those for the photocatalytic reduction of NO_3^-, but in the absence of NO_3^- (see Section 2.4) using the tandem reaction system was 400 μmol (**C**) for 4 h. The amount **C** is consistent with the sum of **A** and **B** (385 μmol). This consistency strongly suggests that the reaction proceeded via a reaction pathway in which H_2 was formed by a photocatalytic reaction over Pt/TiO_2 and the H_2 reduced NO_3^- over $Sn_{0.5}Pd/Al_2O_3$ (Figure 1(a)).

An advantage of the tandem reaction system is that the reaction rates for the photocatalytic H_2 evolution over Pt/TiO_2 and catalytic (non-photocatalytic) NO_3^- reduction over $SnPd/Al_2O_3$

can be controlled appropriately by changing the dose of each catalyst in the reaction mixture. Another advantage is that the Pt/TiO_2 and $SnPd/Al_2O_3$ catalysts can be designed independently to maximize their performance for photocatalytic H_2 evolution and catalytic NO_3^- reduction, respectively. To take advantage of these features, we first investigated the loading amount of Pt on TiO_2 to maximize the photocatalytic performance of Pt/TiO_2.

Figure 3(a) shows the rate of the photocatalytic H_2 evolution over Pt/TiO_2 against the Pt loadings on TiO_2. The reaction was conducted in the presence of glucose but in the absence of both NO_3^- and $SnPd/Al_2O_3$ in the reaction mixture. The dose of Pt/TiO_2 in the reaction mixture was fixed at 200 mg regardless of the Pt loading on TiO_2 and thus the amount of Pt present in the mixture increased with increasing Pt loading. The H_2 evolution rate had two local maxima at 0.5 and 2.3 wt.%. Pt loadings and the maximal activity was obtained at 2.3 wt.%. Thus, 2.3 wt.% Pt/TiO_2 is the best catalyst for photocatalytic H_2 evolution under the present reaction conditions. Ohno et al. have reported that Pt is preferentially photodeposited on TiO_2 particles in rutile rather than anatase phase in the low Pt loading region, if the two crystalline phases are present together in a suspension [37]. This is due to high inherent photocatalytic activity of TiO_2 particles in rutile phase comparing to activity of those in anatase one. In this study, we used P25 as a TiO_2 phototcatalyst, which is known to contain both of these phases. Based on the report by Ohno et al. and the coexistence of two phases, we speculated that the reason for the two local maxima in Figure 3(a) is as follows. For Pt loadings less than 2.0 wt.%, Pt was photodeposited on the TiO_2 particles mainly in the rutile phase and the photocatalytic activity increased with increasing Pt loading up to 0.5 wt.%. However, excess Pt in the rutile phase lowered the photocatalytic activity due to the formation of recombination sites. Thus, for high Pt loadings (> 2.0 wt.%), Pt started to deposit on the TiO_2 particles in the anatase phase and consequently the H_2 evolution rate increased again with Pt loading.

After optimizing the Pt loading for Pt/TiO_2 itself, we then optimized the dose of Pt/TiO_2 in the reaction mixture by using 2.3 wt.% Pt/TiO_2. Photocatalytic H_2 evolution in the glucose

solution without NO_3^- was again used for the optimization. The H_2 evolution rate increased linearly with the increase in the dose of Pt/TiO_2 and reached a maximum at 200 mg (Figure S2). From these results, we fixed the optimal Pt loading on TiO_2 (2.3 wt.% Pt) and dose of Pt/TiO_2 (200 mg) in the reaction mixture for the tandem reaction system under the present reaction conditions.

Next, we attempted to develop a $SnPd/Al_2O_3$ catalyst with high catalytic performance for the reduction of NO_3^- with H_2. It is known that the molar ratio of Pd to a second metal such as Cu is a crucial factor determining the catalytic performance of bimetallic Pd catalysts for the reduction of NO_3^- with H_2 [38–40]. Thus, we optimized the Sn/Pd ratio to obtain $SnPd/Al_2O_3$ with high catalytic activity and high selectivity for gaseous products from the reduction of NO_3^- with H_2. The total amount of metal (sum of Sn and Pd) was fixed at 3 wt.% and thus the loading amounts of both Pd and Sn changed depending on the Sn/Pd ratio. It was found that both Pd and Sn were required for the reduction of NO_3^- with H_2 (Figure S3). The catalytic activity was strongly dependent on the Sn/Pd ratio (Figure S3) and the maximum activity was obtained at Sn/Pd = 0.5, namely $Sn_{0.5}Pd/Al_2O_3$ (1.1 wt.% Sn-1.9 wt.% Pd). Because the rate-limiting step is the reduction of NO_3^- to NO_2^- and this step proceeds on a bimetal site composed of Pd and a second metal [41], it is reasonable that the number of Pd-Sn bimetallic sites on $Sn_{0.5}Pd/Al_2O_3$ was a maximum at Sn/Pd = 0.5. In contrast to its impact on activity, the Sn/Pd ratio had only little impact on the selectivity, as Figure S3 demonstrates. Thus, we concluded that $Sn_{0.5}Pd/Al_2O_3$ was the best catalyst for the reduction of NO_3^- with H_2 in terms of activity as well as selectivity.

We then optimized the dose of $Sn_{0.5}Pd$ bimetal in the reaction mixture for the photocatalytic reduction of NO_3^- by the tandem reaction system. To eliminate the effect on photocatalytic performance due to the shielding effect of Al_2O_3 present in the reaction mixture, the dose of $Sn_{0.5}Pd/Al_2O_3$ in the reaction mixture was fixed at 200 mg and instead the loading amount of $Sn_{0.5}Pd$ bimetal on Al_2O_3 was changed. In Figure 3(b), conversion of NO_3^-,

selectivity for gases ($N_2O + N_2$) and NH_4^+, and the amount of H_2 gas formed are plotted against the loading amount of $Sn_{0.5}Pd$ on Al_2O_3 in the photocatalytic reduction of NO_3^- with the tandem reaction system, where the dose of Pt/TiO_2 in the reaction mixture was fixed at 200 mg. In the absence of $Sn_{0.5}Pd$ (i.e., using bare Al_2O_3), only small amount of NO_3^- was reduced (5% conversion at 4 h), while 684 μmol of H_2 gas was formed because H_2 was not consumed for the reduction of NO_3^-. Conversion of NO_3^- increased with an increase in the loading amount of $Sn_{0.5}Pd$ and reached a maximum at 3 wt.% $Sn_{0.5}Pd$ loading. In contrast, the amount of H_2 gas decreased with increasing $Sn_{0.5}Pd$ loading and only a little H_2 gas evolved when the maximum NO_3^- conversion was obtained at 3 wt.% $Sn_{0.5}Pd$ loading. Under the conditions with the dose of $Sn_{0.5}Pd$ bimetal giving the maximum NO_3^- conversion (3 wt.%), almost all H_2 evolved over Pt/TiO_2 was consumed for the reduction of NO_3^- over $Sn_{0.5}Pd$ bimetal, namely the H_2 evolution rate by the photocatalytic reaction over Pt/TiO_2 was in balance with its consumption rate for NO_3^- reduction over $Sn_{0.5}Pd/Al_2O_3$. Such good balance of the reaction rates of the photocatalytic and thermal catalytic reactions appears to have brought about the high reduction rate of NO_3^-. When the loading amount of $Sn_{0.5}Pd$ on Al_2O_3 exceeded 3 wt.%, the conversion of NO_3^- slightly decreased, probably due to the shielding of Pt/TiO_2 from incident light by $Sn_{0.5}Pd$ particles on Al_2O_3 in the reaction mixture.

As a result of these investigations, the catalytic performance of both Pt/TiO_2 and $Sn_{0.5}Pd/Al_2O_3$ and their doses in the reaction mixture were successfully optimized for the tandem reaction system to give high efficiency in the photocatalytic reduction of NO_3^-.

3.2. Optimization of the single reaction system for photocatalytic reduction of NO_3^-

Before we compare the photocatalytic performance of the tandem reaction system with that of a single reaction system, the photocatalytic performance of the single reaction system should be improved as much as possible. As mentioned in the Introduction, the photocatalytic performance of semiconductor photocatalysts modified with metals (e.g., $SnPd/TiO_2$) depends

strongly on the composition and loading amount of the metals modifying the semiconductor. Thus, the photocatalytic performance of the single reaction system was first upgraded by optimization of both the Sn/Pd ratio and the loading amount of SnPd bimetal on TiO_2 before the comparison.

Figure 4 shows the influence of the Sn/Pd ratio and loading amount on the photocatalytic performance for NO_3^- reduction. The total number of electrons consumed for both photocatalytic NO_3^- reduction and H_2 evolution, calculated from the amounts of all products (NO_2^-, N_2O, N_2, and NH_4^+) and the amount of H_2 gas evolved at 4 h based on eqs. 6-10, is shown in Figure 4(a).

$$NO_3^- + 2e^- + 2H^+ \rightarrow NO_2^- + H_2O \quad (6)$$

$$NO_3^- + 4e^- + 5H^+ \rightarrow 1/2N_2O + 5/2H_2O \quad (7)$$

$$NO_3^- + 5e^- + 6H^+ \rightarrow 1/2N_2 + 3H_2O \quad (8)$$

$$NO_3^- + 8e^- + 10H^+ \rightarrow NH_4^+ + 3H_2O \quad (9)$$

$$2H^+ + 2e^- \rightarrow H_2 \quad (10)$$

The total number of electrons is denoted by $\mathbf{N}\boldsymbol{e}^-$ and is a measure representing the total photocatalytic activity of $SnPd/TiO_2$. Roughly, catalysts with a low Sn/Pd ratio and low loading amounts of SnPd bimetal had large $\mathbf{N}\boldsymbol{e}^-$. $Sn_{0.5}Pd/TiO_2$ with Sn/Pd = 0.5 and 1 wt.% $Sn_{0.5}Pd$ loading gave the maximum $\mathbf{N}\boldsymbol{e}^-$ (1416 μmol). The decrease of $\mathbf{N}\boldsymbol{e}^-$ with an increase in the loading amount for the same Sn/Pd ratio was probably because excess SnPd metals on TiO_2 blocked incident light or provided recombination sites for photoexcited electrons (e^-) and holes (h^+).

The ratio of electrons consumed for NO_3^- reduction to $\mathbf{N}\boldsymbol{e}^-$ is defined as the selectivity for NO_3^- reduction ($\mathbf{NO_3^-\_}\boldsymbol{e}^-$) here. $\mathbf{NO_3^-\_}\boldsymbol{e}^-$ was calculated from eq. 11, where $Y(product)$ is the

yield of each product over 4 h and the coefficient for each yield in eq. 11 is the number of electrons necessary for the reduction to give each product (eqs. 6-9). The yields of N_2 and N_2O are calculated based on the amount of NO_3^- consumed.

$$\mathbf{NO_3^-\_}\boldsymbol{e}^- \ (\%) = \frac{2Y(NO_2^-) + 4Y(N_2O) + 5Y(N_2) + 8Y(NH_4^+)}{\mathbf{N}e^-} \times 100 \quad (11)$$

If $\mathbf{NO_3^-\_}\boldsymbol{e}^-$ is 100%, all photoexcited electrons are consumed for NO_3^- reduction and no electrons are consumed for H_2 evolution. Figure 4(b) shows the influence of the Sn/Pd ratio and the loading amount of SnPd bimetal on $\mathbf{NO_3^-\_}\boldsymbol{e}^-$. $\mathbf{NO_3^-\_}\boldsymbol{e}^-$ increased with an increase in the Sn/Pd ratio as well as the loading amount: that is, photoexcited electrons were preferentially consumed for NO_3^- reduction rather than H_2 evolution over SnPd/TiO_2 with a high Sn/Pd ratio and large SnPd loading. Because NO_3^- is activated on Sn or Sn-Pd sites [38], the high Sn/Pd ratio and large SnPd bimetal loading are beneficial for preferential consumption of photoexcited electrons for NO_3^- reduction.

Actually, the single reaction system (SnPd/TiO_2) promoted the photocatalytic reduction of NO_3^-, but photocatalytic H_2 evolution still proceeded because there was low $\mathbf{NO_3^-\_}\boldsymbol{e}^-$ for the catalysts with low Sn/Pd ratio and low SnPd loading, giving large $\mathbf{N}\boldsymbol{e}^-$ (Figure 4(a)). For the single reaction system, it is inevitable that both NO_3^- reduction and H_2 evolution proceed over the SnPd metals on TiO_2 in parallel, though it is readily expected that NO_3^- reduction is much easier than H_2 evolution based on the reduction potentials for each reaction ($E°(H^+/H_2)$ = 0 V vs. SHE, $E°(NO_3^-/NO_2^-)$ = +0.84 V vs. SHE, $E°(NO_3^-/NH_4^+)$ = +0.88 V vs. SHE, $E°(NO_3^-/N_2O)$ = +1.12 V vs. SHE, and $E°(NO_3^-/N_2)$ = +1.25 V vs. SHE).

In a separate experiment, the non-photocatalytic (i.e., catalytic) performance of SnPd/TiO_2 was evaluated for the catalytic reduction of NO_3^- with H_2 in water in the dark. It was found that catalytic activity increased with an increase in the Sn/Pd ratio as well as with an increase in the

SnPd loadings (Figure S4(a)). This response to the Sn/Pd ratio and loading amount was very similar to that of $\mathbf{NO_3^-\_}\boldsymbol{e}^-$ shown in Figure 4(b).

The conversion of NO_3^- greatly increased with increasing SnPd loading for the photocatalytic reduction of NO_3^- (Figure 4(c)). Although the optimal Sn/Pd ratio differed depending on the loading amount, $SnPd/TiO_2$ with Sn/Pd = 2 showed high NO_3^- conversion. While the Sn/Pd ratio had only a small impact on the selectivity, the catalyst with Sn/Pd =2 showed the highest selectivity for gas (N_2O and N_2) as shown in Figure 4(d)).

Although SnPd bimetal is necessary for the activation of NO_3^-, as Figure 4(c) demonstrates, it is expected that excess SnPd bimetal on TiO_2 shields TiO_2 from incident light. Thus, the optimization of the loading amount of Sn_2Pd bimetal (Sn/Pd = 2) on TiO_2 is necessary to develop a single reaction system with high photocatalytic performance. Figure 5(a) shows the influence of the loading amount of Sn_2Pd bimetal on TiO_2 for photocatalytic NO_3^- reduction over the single reaction system (Sn_2Pd/TiO_2). Though bare TiO_2 showed activity for photocatalytic NO_3^- reduction, most of the product was undesirable NH_4^+. The photocatalytic activity of bare TiO_2 is consistent with previous reports [10, 11, 29, 42–44], while some papers show no activity of bare TiO_2 [45, 46] maybe due to different reaction conditions and hole scavengers. Modification of TiO_2 with a small amount of Sn_2Pd bimetal drastically improved $\mathbf{N}\boldsymbol{e}^-$ and it reached a maximum of 1.2 mmol at 0.5 wt.% Sn_2Pd loading (Figure 5(b)), indicating that Sn_2Pd/TiO_2 with 0.5 wt.% Sn_2Pd loading had the highest photocatalytic activity. However, as Figure 5(c) shows, the rise in NO_3^- conversion by modification with 0.5 wt.% Sn_2Pd was not large in comparison with the bare TiO_2 (0 wt.%) conversion. That is, a vast majority of photoexcited electrons moving to the surface of 0.5 wt.% Sn_2Pd/TiO_2 were consumed for H_2 evolution. In fact, $\mathbf{NO_3^-\_}\boldsymbol{e}^-$ was only 21% for 0.5 wt.% Sn_2Pd/TiO_2 (Figure 5(b)). The maximum NO_3^- conversion was obtained at 1 wt.% Sn_2Pd loading. In addition, the 1 wt.% Sn_2Pd catalyst showed the highest selectivity for gas ($N_2O + N_2$) (73%, Figure 5(a)).

Figure 5(c) shows influence of the Sn_2Pd loading on TiO_2 for non-photocatalytic reduction

of NO_3^- with H_2 over Sn_2Pd/TiO_2 in the dark. The activity increased monotonically with increasing Sn_2Pd loading. In the range of the Sn_2Pd loadings that were investigated in this study (up to 3wt.%), the catalyst with 3 wt.% Sn_2Pd showed the highest activity for NO_3^- reduction. The selectivity for gas (N_2O + N_2) also increased with increasing Sn_2Pd loading, but the changes were not very large. The dependence of the selectivity for gas on the Sn_2Pd loadings were different for the photocatalytic NO_3^- reduction (Figure 5(a)) and the non-photocatalytic reaction with H_2 (Figure 5(c)). In the case of photocatalytic reduction, the maximum selectivity for gas was obtained with 1 wt.% Sn_2Pd loading, whereas the selectivity increased monotonically against the Sn_2Pd loading for the non-photocatalytic reduction. In the photocatalytic reaction, the photoexcited electrons generated in TiO_2 transferred to Pd sites and then reduced H^+ or H_2O to form atomic hydrogen on the Pd sites. Consequently, atomic hydrogen is likely to form on the Pd sites, on which the photoexcited electrons tend to concentrate. On the other hand, in non-photocatalytic NO_3^- reduction with H_2, atomic hydrogen was formed on Pd sites that have a high capacity for dissociative adsorption of H_2. Since reduction of NO_3^- proceeds on those Pd sites by reaction with the atomic hydrogen, the properties of the Pd sites must be crucial in determining the selectivity. It is presumably the case that the properties of the Pd sites on which the photoexcited electrons tend to concentrate are different from those having a high capacity for the dissociative adsorption of H_2. Thus, we speculate that this difference in the properties of the Pd sites resulted in different trends in the selectivity against the Sn_2Pd loadings for photocatalytic and non-photocatalytic NO_3^- reductions.

As Figure 5(b) clearly shows, the total photocatalytic activity ($\mathbf{N}\boldsymbol{e}^-$) of the single reaction system had a maximum at 0.5 wt.% Sn_2Pd loading. In contrast, a larger Sn_2Pd loading always means a higher capacity for the activation of NO_3^- on the Sn_2Pd metal through adsorption, as Figure 5(c) indicates. Namely, the optimal Sn_2Pd loading is mismatched between the total photocatalytic activity and capacity for the NO_3^- activation via adsorption for the single reaction

system. Eventually, the maximum photocatalytic activity for NO_3^- reduction was obtained at the 1 wt.% Sn_2Pd loading, representing a compromise for total photocatalytic activity and capacity for NO_3^- activation via adsorption under the present reaction conditions.

3.3. Comparison of tandem and single reaction systems for photocatalytic reduction of NO_3^- in water

Through the investigations described in Sections 3.1 and 3.2, the photocatalytic performance was maximized for both the tandem and the single reaction systems. Next, we compared the systems for the photocatalytic reduction of NO_3^- in water. Figure 6 shows time courses for the photocatalytic reduction of NO_3^- in water over the tandem and single reaction systems, where the conversion of NO_3^-, along with the selectivities for gas (N_2O + N_2) and NH_4^+, $\mathbf{N}\boldsymbol{e}^-$, and $\mathbf{NO_3^-}\boldsymbol{\_e^-}$. Figure 6(a) clearly demonstrates that the tandem reaction system was highly superior in the conversion of NO_3^- and selectivity for gas. In the tandem reaction system all of the NO_3^- was reduced at 24 h and the selectivity for gas was more than 94% regardless of the conversion of NO_3^-. In contrast, in the single reaction system the selectivity for gas products was around 70% and 40 h or more was necessary to achieve complete NO_3^- reduction.

It should be noted that $\mathbf{NO_3^-}\boldsymbol{\_e^-}$ for the tandem reaction system was much higher than that for the single reaction system (Figure 6(b)). The tandem system gave an extremely high $\mathbf{NO_3^-}\boldsymbol{\_e^-}$ of more than 95% until the NO_3^- conversion reached 85% at 12 h, meaning that the photoexcited electrons were preferentially consumed for the NO_3^- reduction. On the other hand, $\mathbf{NO_3^-}\boldsymbol{\_e^-}$ was less than 60% for the single reaction system even in the low NO_3^- conversion region, meaning that the photoexcited electrons were wasted in order to evolve H_2 by the reduction of H^+ or H_2O in water. From these results, we conclude that the tandem reaction system is an excellent photocatalytic reaction system that can promptly and selectively reduce NO_3^- to gaseous products in water under irradiation without photocatalytic H_2 evolution. This is because Pt/TiO_2 and $SnPd/Al_2O_3$ catalysts can be designed independently to maximize the

performance of each in the tandem reaction system and the optimal dose of each catalyst in the reaction mixture can be determined. These are the special advantages that the single reaction system lacks.

4. Conclusions

The tandem reaction system consisting of Pt/TiO_2 and $SnPd/Al_2O_3$ dispersed in water has two advantages: (i) Pt/TiO_2 and $SnPd/Al_2O_3$ catalysts can be designed independently to have high photocatalytic and catalytic performance, respectively; and (ii) the rates of the photocatalytic and catalytic reactions can be easily controlled by changing catalyst doses in a reactor. To demonstrate these advantages, a systematic optimization of the tandem reaction system has been conducted and been compared with an optimized $SnPd/TiO_2$ single reaction system. The tandem reaction system with the optimal loading amount of Pt on TiO_2, optimal Sn/Pd ratio and loading amount of SnPd on Al_2O_3, and optimal doses of the two catalysts produced a high reduction rate of NO_3^- and high selectivity for gas (94%) under light irradiation ($\lambda > 300$ nm) in the presence of glucose as a hole scavenger. On the other hand, the single reaction system with an optimized Sn/Pd ratio and loading amount of SnPd bimetal on TiO_2 reduced NO_3^- about two-thirds as fast as the tandem reaction system, and was less selective for gas products (70%). In addition, the tandem reaction system had a high light use efficiency for NO_3^- reduction (95%) by photocatalytic reduction (which is defined as a ratio of the electrons consumed for NO_3^- reduction to the total number of electrons consumed for both NO_3^- reduction and photocatalytic H_2 evolution) compared with that in the single reaction system, though the total number of electrons was about the same in each case. The high light use efficiency for the NO_3^- reduction, which was brought about by the advantages of the tandem reaction system, led to the prompt reduction of NO_3^- in the system.

Acknowledgement

This work was supported by JSPS KAKENHI Grant Number 15J05423.

References

[1] K. Sayama, H. Arakawa, J. Chem. Soc., Faraday Trans. 93 (1997) 1647–1654.

[2] S. Tabata, N. Nishida, Y. Masaki, K. Tabata, Catal. Lett. 34 (1995) 245–249.

[3] H. Kotani, R. Hanazaki, K. Ohkubo, Y. Yamada, S. Fukuzumi, Chem.–Eur. J. 17 (2011) 2777–2785.

[4] S. Chen, Y. Qi, Q. Ding, Z. Li, J. Cui, F. Zhang, C. Li, J. Catal. 339 (2016) 77–83.

[5] S. Shibuya, S. Aoki, Y. Sekine, I. Mikami, Appl. Catal. B Environ. 138–139 (2013) 294–298.

[6] O. Tomita, T. Otsubo, M. Higashi, B. Ohtani, R. Abe, ACS Catal. 6 (2016) 1134–1144.

[7] J. Sá, M. Fernández-García, J.A. Anderson, Catal. Commun. 9 (2008) 1991–1995.

[8] A.M. Lacerda, I. Larrosa, S. Dunn, Nanoscale 7 (2015), 12331–123355.

[9] S.K. Mohapatra, N. Kondamudi, S. Banerjee, M. Misra, Langmuir 24 (2008) 11276–11281.

[10] H. Kominami, H. Gekko, K. Hashimoto, Phys. Chem. Chem. Phys. 12 (2010) 15423–15427.

[11] F. Zhang, R. Jin, J. Chen, C. Shao, W. Gao, L. Li and N. Guan, J. Catal. 232 (2005) 424–431.

[12] K. Domen, S. Naito, M. Soma, T. Onishi, K. Tamura, J. Chem. Soc., Chem. Commun. (1980) 543–544.

[13] K. Domen, A. Kudo, T. Onishi, N. Kosugi, H. Kuroda, J. Phys. Chem. 90 (1986) 292–295.

[14] H. Kato, K. Asakura, A. Kudo, J. Am. Chem. Soc. 125 (2003) 3082–3089.

[15] H. Husin, W.-N. Su, H.-M. Chen, C.-J. Pan, S.-H. Chang, J. Rick, W.-T. Chuang, H.-S. Sheu, B.-J. Hwang, Green Chem. 13 (2011) 1745–1754.

[16] A. K. Agegnehu, C.-J. Pan, J. Rick, J.-F. Lee, W.-N. Su, B.-J. Hwang, J. Mater. Chem. 22

(2012) 13849–13854.

[17] K. Maeda, K. Teramura, H. Masuda, T. Takata, N. Saito, Y. Inoue, K. Domen, J. Phys. Chem. B 110 (2006) 13107–13112.

[18] K. Maeda, H. Hashiguchi, H. Masuda, R. Abe, K. Domen, J. Phys. Chem. C 112 (2008) 3447–3452.

[19] T. Hisatomi, K. Maeda, K. Takanabe, J. Kubota, K. Domen, J. Phys. Chem. C 113 (2009) 21458–21466.

[20] K. Iizuka, T. Wato, Y. Miseki, K. Saito, A. Kudo, J. Am. Chem. Soc. 133 (2011) 20863–20868.

[21] T. Takayama, K. Tanabe, K. Saito, A. Iwase, A. Kudo, Phys. Chem. Chem. Phys. 16 (2014) 24417–24422.

[22] M. Yamamoto, T. Yoshida, N. Yamamoto, T. Nomoto, Y. Yamamoto, S. Yagi, H. Yoshida, J. Mater. Chem. A 3 (2015) 16810–16816.

[23] H. Kominami, T. Nakaseko, Y. Shimada, A. Furusho, H. Inoue, S. Murakami, Y. Kera, B. Ohtani, Chem. Commun. (2005) 2933–2935.

[24] O.S.G.P. Soares, M.F.R. Pereira, J.J.M. Órfao, J.L. Faria, C.G. Silva, Chem. Eng. J. 251 (2014) 123–130.

[25] D. Yang, W. Feng, G. Wu, L. Li, N. Guan, Catal. Today 175 (2011) 356–361.

[26] N. Wehbe, M. Jaafar, C. Guillard, J.M. Herrmann, S. Miachon, E. Puzenat, N. Guilhaume, Appl. Catal. B General 368 (2009) 1–8.

[27] J.A. Anderson, Catal. Today 175 (2011) 316–321.

[28] J.A. Anderson, Catal. Today 181 (2012) 171–176.

[29] J. Sá, C.A. Agüera, S. Gross, J.A. Anderson, Appl. Catal. B Environ. 85 (2009) 192–200.

[30] R. Lucchetti, L. Onotri, L. Clarizia, F.D. Natale, I.D. Somma, R. Andreozzi, R. Marotta, Appl. Catal. B Environ. 202 (2017) 539–549.

[31] K. Sayama, K. Mukasa, R. Abe, Y. Abe, H. Arakawa, Chem. Commun. (2001) 2416–2417.

[32] R. Abe, K. Sayama, H. Sugihara, J. Phys. Chem. B 109 (2005) 16052–16061.

[33] Q. Jia, A. Iwase, A. Kudo, Chem. Sci. 5 (2014) 1513–1519.

[34] J. Hirayama, H. Kondo, Y. Miura, R. Abe, Y. Kamiya, Catal. Commun. 20 (2012) 99–102.

[35 J. Hirayama, Y. Kamiya, ACS Catal. 4 (2014) 2207–2215.

[36] J. Hirayama, R. Abe, Y. Kamiya, Appl. Catal. B Environ. 144 (2014) 721–729.

[37] T. Ohno, K. Sarukawa, M. Matsumura, New J. Chem. 26 (2002) 1167–1170.

[38] U. Prüsse, K.-D. Vorlop, J. Mol. Catal. A Chem. 173 (2001) 313-328.

[39] Y. Yoshinaga, T. Akita, I. Mikami, T. Okuhara, J. Catal. 207 (2002) 37–45.

[40] M. Al Bahri, L. Calvo, M.A. Gilarranz, J.J. Rodriguez, F. Epron, Appl. Catal. B Environ. 138–139 (2013) 141–148.

[41] J. Sa, N. Barrabes, E. Kleymenov, C. Lin, K. Fottinger, O.V. Safonova, J. Szlachetko, J.A. van Bokhoven, M. Nachtegaal, A. Urakawa, G.A. Crespo, G. Rupprechter, Catal. Sci. Technol. 2 (2012) 794–799.

[42] K.D. Doudrick, O. Monzon, A. Mangonon, K. Hristovski, P. Westerhoff, J. Environ. Eng. 138 (2012) 852–861.

[43] B. Bems, F.C. Jentoft, R. Schlögl, Appl. Catal. B Environ. 20 (1999) 155–163.

[44] Y. Li, F. Wasgestian, J. Photochem. Photobiol. A: Chem. 112 (1998) 255–259.

[45] R. Jin, W. Gao, J. Chen, H. Zeng, F. Zhang, Z. Liu, N. Guan, J. Photochem. Photobiol. A: Chem. 162 (2004) 585–590.

[46] M.M. Mohamed, B.H.M. Asghar, H.A. Muathen, Catal. Commun. 28 (2012) 58–63.

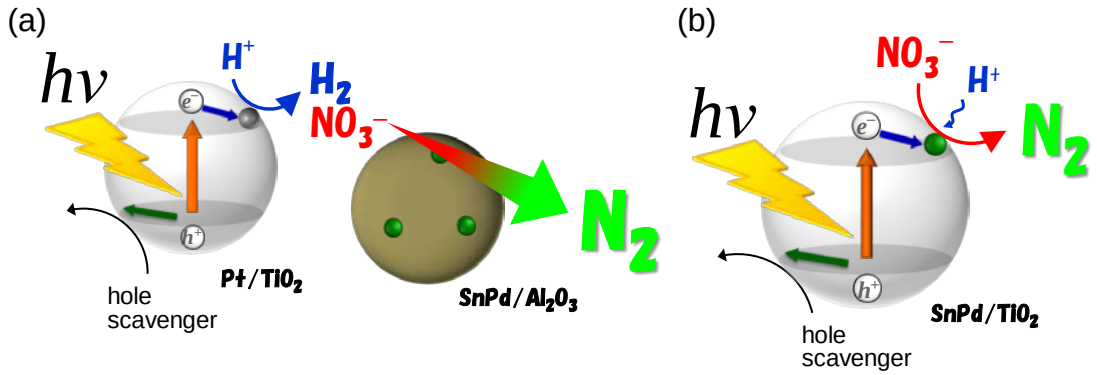

Figure 1 Schematic images of (a) a tandem reaction system and (b) a single reaction system.

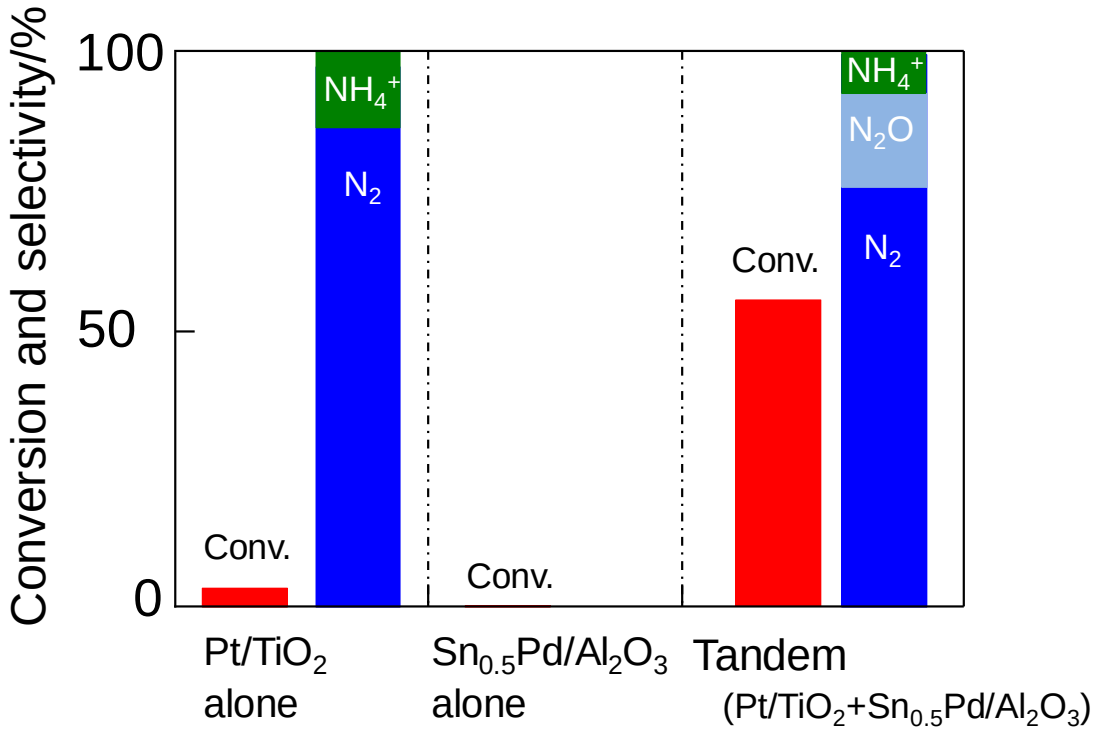

Figure 2 Photocatalytic reductions for 4 h of NO_3^- over 2.3 wt.% Pt/TiO_2 alone, 3.0 wt.% $Sn_{0.5}Pd/Al_2O_3$ alone, and a tandem reaction system. Left (red) and right (blue, light blue, and green) bars represent conversion and selectivity, respectively. Reaction conditions: catalyst dose, 2.3 wt.% Pt/TiO_2, 200 mg, 3.0 wt.% $Sn_{0.5}Pd/Al_2O_3$, 200 mg; reactant NO_3^- (from KNO_3), 1.0 mmol dm^{-3} with 100 mmol dm^{-3} glucose; reaction volume, 250 cm^3; light source, 300 W Xe lamp ($\lambda > 300$ nm); and reaction time, 4 h.

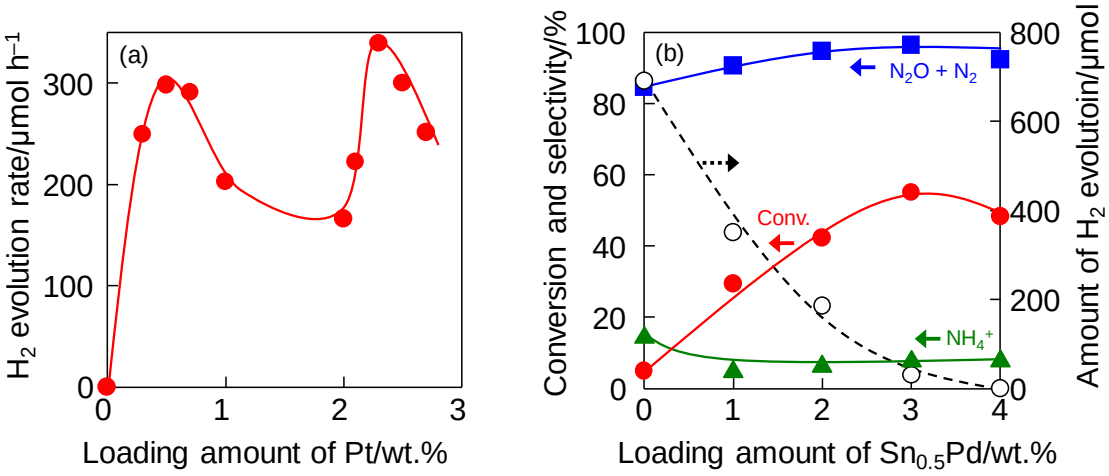

Figure 3 Optimization of loading amounts of (a) Pt on TiO_2 and (b) $Sn_{0.5}Pd$ on Al_2O_3. The reactions used for the optimizations were photocatalytic H_2 evolution in aqueous glucose solution over Pt/TiO_2 for (a) and photocatalytic NO_3^- reduction in the presence of 2.3 wt.% Pt/TiO_2 and *x* wt.% $Sn_{0.5}Pd/Al_2O_3$ for (b). The amount of $Sn_{0.5}Pd/Al_2O_3$ added to the reaction mixture was fixed at 200 mg regardless of x wt.% for experiment (b). Reaction conditions for (a): catalyst weight, 0–2.7 wt.% Pt/TiO_2, 200 mg; 100 mmol L^{-1} glucose; volume of reaction mixture, 250 cm^3; light source, 300 W Xe lamp (λ > 300 nm); and reaction time, 1 h. Reaction conditions for (b): catalyst weight, 2.3 wt.% Pt/TiO_2, 200 mg and *x* wt.% $Sn_{0.5}Pd/Al_2O_3$, 200 mg; reactant NO_3^- (from KNO_3), 1.0 mmol dm^{-3} with 100 mmol dm^{-3} glucose; volume of reaction mixture, 250 cm^3; light source, 300 W Xe lamp (λ > 300 nm); and reaction time 4 h.

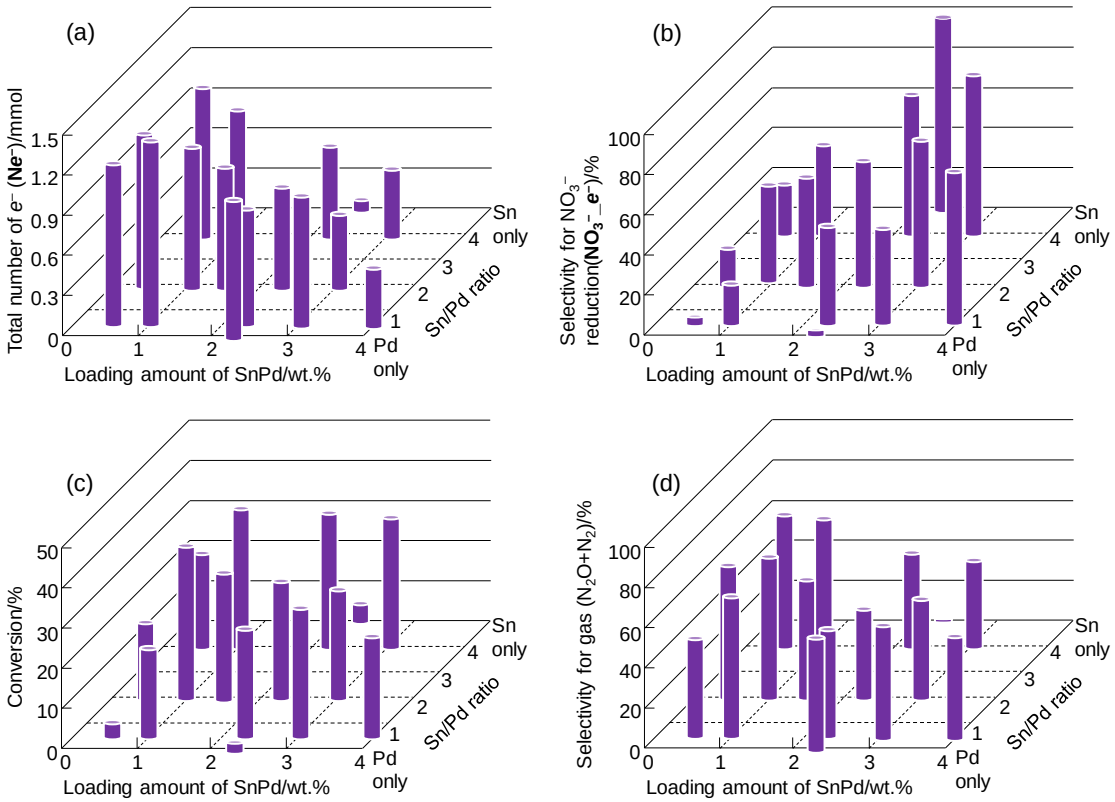

Figure 4 Influence of loading amount of SnPd and Sn/Pd ratio on (a) number of e^- consumed for the reactions, (b) selectivity for NO_3^- reduction ($\mathbf{NO_3^-\_e^-}$), (c) conversion of NO_3^-, and (d) selectivity for the sum of N_2O and N_2 over Sn_nPd/TiO_2 for the photocatalytic reduction of NO_3^- in water. Reaction conditions: catalyst weight, Sn_nPd/TiO_2, 200 mg; reactant NO_3^- (from KNO_3), 1.0 mmol dm^{-3} with 100 mmol dm^{-3} glucose; reaction volume, 250 cm^3; light source, 300 W Xe lamp ($\lambda > 300$ nm); and reaction time, 4 h.

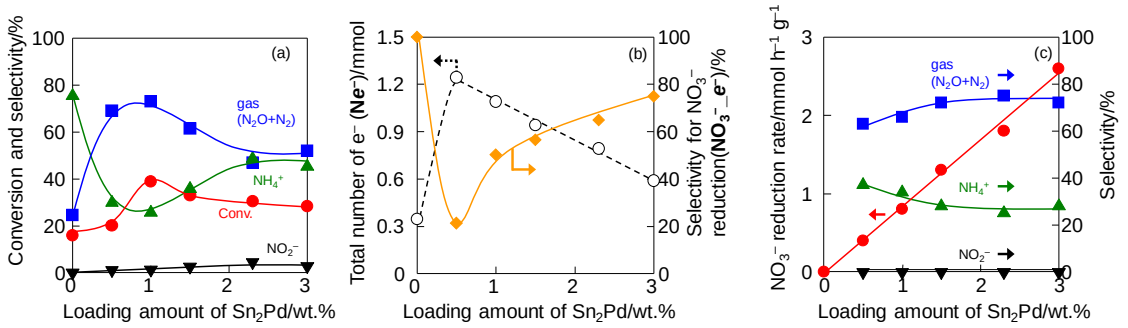

Figure 5 Influence of Sn_2Pd loading on (a and b) photocatalytic NO_3^- reduction over x wt.% Sn_2Pd/TiO_2 and (c) catalytic reduction of NO_3^- with H_2 over x wt.% Sn_2Pd/TiO_2. Reaction conditions: (a and b) catalyst weight, x wt.% Sn_2Pd/TiO_2, 200 mg; reactant NO_3^- (from KNO_3), 1.0 mmol dm^{-3} with 100 mmol dm^{-3} glucose; volume of reaction mixture, 250 cm^3; light source, 300 W Xe lamp ($\lambda > 300$ nm); and reaction time, 4 h. (c) catalyst weight, x wt.% Sn_2Pd/TiO_2, 50 mg; reactant NO_3^- (from KNO_3), 1.0 mmol dm^{-3}; volume of reaction mixture, 250 cm^3; gas composition, H_2/CO_2 = 1/1; gas flow rate, 30 cm^3 min^{-1}; and reaction time, 1 h.

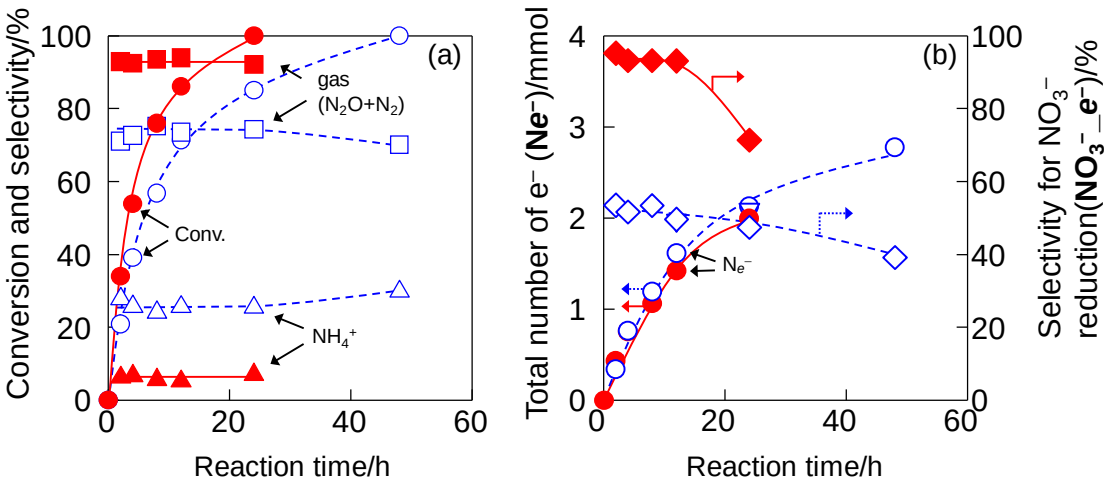

Figure 6 Comparison of a tandem reaction system with a single reaction system for photocatalytic NO_3^- reduction in water. Red and blue symbols represent the tandem and single reaction systems, respectively. (a) Conversion of NO_3^- and selectivity for NO_2^-, NH_4^+, and gas (N_2O + N_2). (b) Total number of e^- (**N*e*$^-$**) and selectivity for NO_3^- reduction (**NO_3^-_*e*$^-$**). Reaction conditions: catalyst weight, 2.3 wt.% Pt/TiO_2, 200 mg and 3.0 wt.% $Sn_{0.5}Pd/Al_2O_3$, 200 mg; 1 wt.% Sn_2Pd/TiO_2, 200 mg; reactant NO_3^- (from KNO_3), 1.0 mmol dm^{-3} with 100 mmol dm^{-3} glucose; reaction volume, 250 cm^3; and light source, 300 W Xe lamp (λ > 300 nm).

Supplementary Information

Highly selective and efficient photocatalytic reduction of nitrate in water by a tandem reaction system consisting of Pt/TiO_2 and $SnPd/Al_2O_3$: A comparative study of the tandem reaction system with a usual semiconductor photocatalyst $SnPd/TiO_2$

Jun Hirayama[a,b] and Yuichi Kamiya[c,*]

[a] Faculty of Environmental Earth Science, Hokkaido University, Nishi 5, Kita 10, Kita-ku, Sapporo, Hokkaido 060-0810, Japan

[b] Research Fellow of Japan Society for the Promotion of Science (JSPS), 5-3-1 Chiyoda-ku, Tokyo 102-0083, Japan

[*]Corresponding author

Yuichi Kamiya

E-mail: kamiya@ees.hokudai.ac.jp, Tel/Fax: +81-11-706-2217

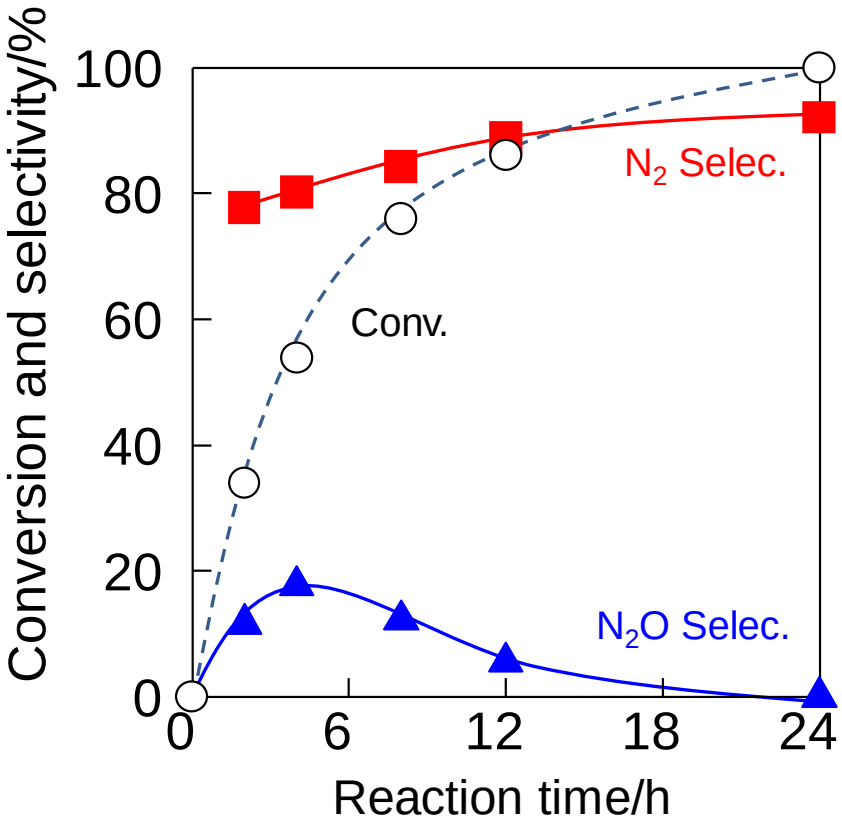

Figure S1. Time courses for (○) conversion of NO_3^- and selectivities for (■) N_2 and (▲) N_2O over a tandem reaction system. Reaction conditions: catalyst weight, 2.3 wt.% Pt/TiO_2, 200 mg and 3.0 wt.% $Sn_{0.5}Pd/Al_2O_3$, 200 mg; reactant NO_3^- (from KNO_3), 1.0 mmol dm^{-3} with 100 mmol dm^{-3} glucose; reaction volume, 250 cm^3; and light source, 300 W Xe lamp ($\lambda > 300$ nm).

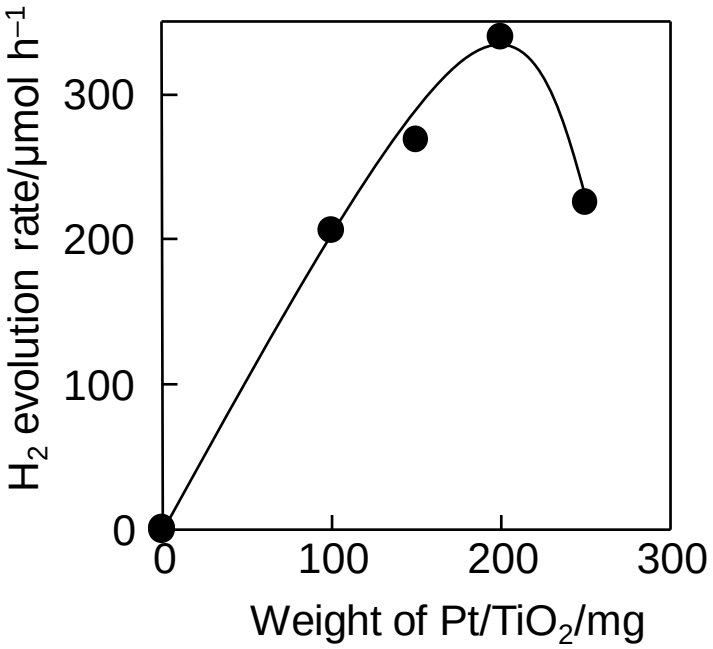

Figure S2 Dependence of H_2 evolution rate over Pt/TiO_2 under light irradiation ($\lambda > 300$ nm) on the weight of Pt/TiO_2 loaded in the reaction mixture. The H_2 evolution rate was estimated from the amount of H_2 formed at 1 h after the beginning of the reaction. Reaction conditions: reaction mixture, 100 mmol dm^{-3} aqueous glucose solution (250 cm^3), and light source, 300 W Xe lamp ($\lambda > 300$ nm). $Sn_{0.5}Pd/Al_2O_3$ was not loaded in the reactor, and NO_3^- was not present in the reaction mixture.

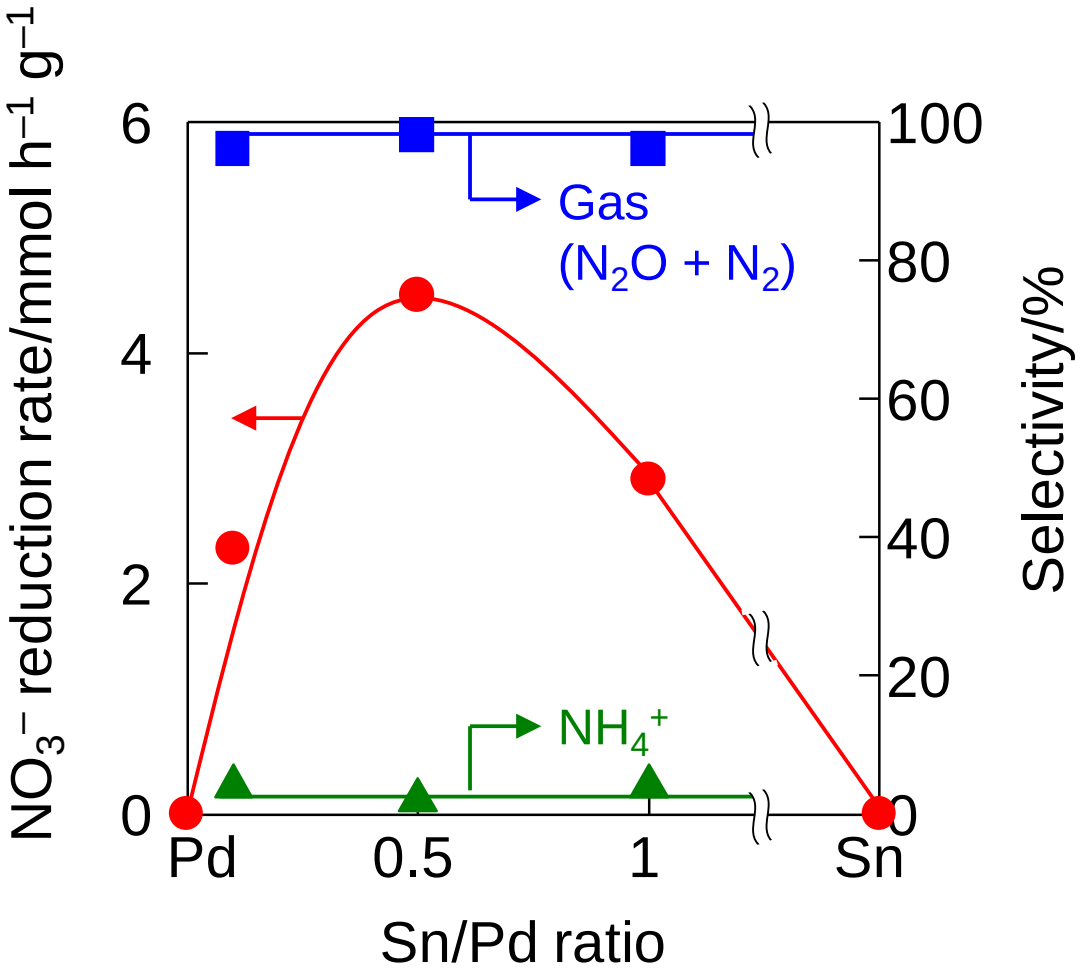

Figure S3 Influence of Sn/Pd ratio on (●) NO_3^- reduction rate and selectivity for (■) gas and (▲) NH_4^+ over Sn_nPd_m/Al_2O_3 for the catalytic hydrogenation of NO_3^- with H_2 in water. Reaction conditions: catalyst weight, 3 wt.% Sn_nPd/Al_2O_3, 30 mg; reactant NO_3^- (from KNO_3), 1.0 mmol dm^{-3}; volume of reaction mixture, 250 cm^3; gas composition, H_2/CO_2 = 1/1; and gas flow rate, 30 cm^3 min^{-1}. Pt/TiO_2 was not loaded in the reactor, and glucose was not present in the reaction mixture.

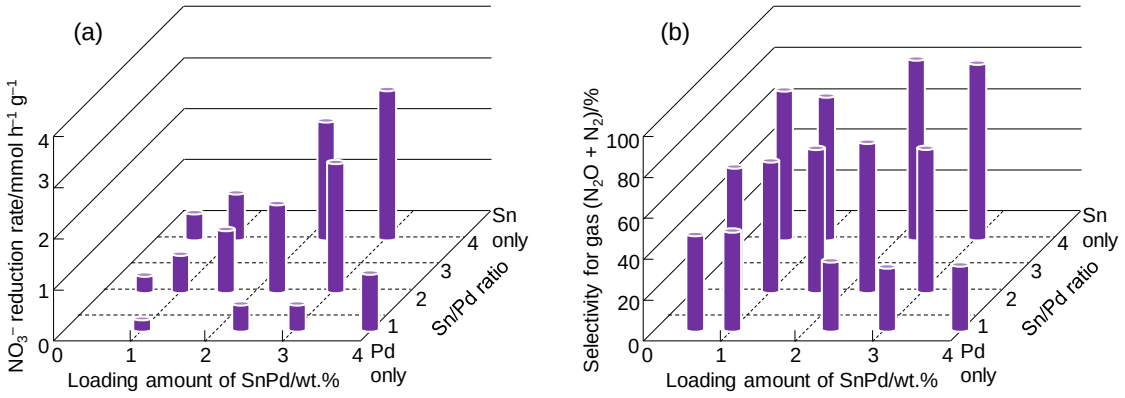

Figure S4 Influence of loading amount of SnPd and Sn/Pd ratio on (a) NO_3^- reduction rate and (b) selectivity for gas over Sn_nPd/TiO_2 for catalytic reduction of NO_3^- in water under dark conditions. Reaction conditions: catalyst weight, Sn_nPd/TiO_2 50 mg; reactant NO_3^- (from KNO_3), 1.0 mmol dm^{-3}; volume of reaction mixture, 250 cm^3; gas composition, H_2/CO_2 = 1/1; and total gas flow rate, 30 cm^3 min^{-1}.